UNCLASSIFIED

1

AECD-3816

Subject Category: PHYSICS

UNITED STATES ATOMIC ENERGY COMMISSION

THE EFFECTIVE XENON CROSS SECTION

By
H. L. Garabedian
R. R. Schiff

September 1954

Atomic Power Division
Westinghouse Electric Corporation
Pittsburgh, Pennsylvania

Technical Information Service, Oak Ridge, Tennessee

UNCLASSIFIED

DISCLAIMER

Date Declassified: December 6, 1955.

Printed in USA, Price 30 cents. Available from the Office of Technical Services, Department of Commerce, Washington 25, D. C.

AECD-3816

THE EFFECTIVE XENON CROSS SECTION

By
H. L. Garabedian
R. R. Schiff

September 1954

Work performed under Contract No. AT-11-1-Gen-14.

Atomic Power Division
Westinghouse Electric Corporation
Pittsburgh, Pennsylvania

TABLE OF CONTENTS

THE EFFECTIVE XENON CROSS SECTION

ABSTRACT

The notion of effective xenon cross section, as defined in WAPD-RM-128, has been reassessed in the light of several recent advances in reactor theory: (i) use of the window-shade theory, exemplified in WAPD-RM-210, in studying partially inserted groups of control rods, (ii) use of the one-dimensional multiregion analogue machine (the GODDESS) in solving criticality problems with a variable absorption cross section, (iii) use of new techniques in evaluating an improved formulation of the effective xenon cross section. The definition of effective xenon cross section appears not only in the maximum xenon override problem but also in the temperature coefficient problem at the time of maximum xenon override, and differences in the interpretation of the definition in these two problems are discussed in detail.

Two examples are studied in detail which illustrate the improved techniques developed in this paper for the evaluation of the effective xenon cross section in the maximum xenon override problem. Both examples serve to illustrate the striking effect of the preshutdown power level on the thermal flux distribution at the time of maximum xenon override and reveal convincingly earlier misconceptions on the problem.

THE EFFECTIVE XENON CROSS SECTION

H. L. Garabedian and R. R. Schiff

1. Introduction

The notion of effective xenon cross section first presented itself at the Westinghouse Atomic Power Division in connection with the xenon override problem. The need for such a definition arises from the inhomogeneous distribution of xenon (and samarium) at the time of shutdown and the subsequent use of homogeneous reactor theory in the study of the transient xenon problem. The definition of effective xenon cross section and early applications of the definition are contained in WAPD-RM-128.

By effective xenon cross section is meant that cross section associated with a homogeneous distribution which is the reactivity equivalent of the actual non-uniformly distributed xenon. The mathematical formulation of effective xenon cross section is effected with the aid of the generalized reactivity formula (Nordheim perturbation formula[**]). In this formulation, the unperturbed flux is taken as the flux in the reactor at the time of maximum xenon override with a homogeneous distribution of xenon poison; the perturbed flux is the flux in the reactor at the time of maximum xenon override arising from the preshutdown distribution of xenon in its actual inhomogeneous state. At the time of publication of WAPD-RM-128 it was assumed that the perturbed flux was very little

---

** H. L. Garabedian, Theory of Homogeneous Control of a Cylindrical Reactor, WAPD-19, September 1950.

different from and indeed, to a first order approximation, taken to coincide with the unperturbed flux. This constraint was a necessity since it was impossible to obtain flux distributions in a reactor with a continuously varying reactor parameter with the use of analytic methods and desk machine calculations. Moreover, it was generally supposed at the time that the perturbation under discussion was very small and hence that it was unnecessary to know the actual form of the perturbed flux.

It is now possible, with the aid of the analogue machine called the GODDESS,* to solve one-dimensional multiregion reactor problems, where the reactor parameters may vary continuously. In particular, it has recently been discovered that in the operating range of power levels of the Mark I STR the flux perturbation described above is substantial rather than very small. It is thus the first object of this report to reassess past calculations of the effective xenon cross section and to investigate new techniques of calculating this reactor parameter in the light of substantial perturbations and also the operating rod configurations.

The notion of effective xenon cross section appears again in reactor theory in connection with the problem of calculating the temperature coefficient of reactivity at the time of override of maximum xenon. In this situation, however, the interpretation of effective xenon cross section differs from that encountered in the xenon override problem. In view of such a difference in interpretation in the two problems, an additional objective of this paper is to discuss the role of the generalized reactivity formula in the temperature coefficient problem and, in particular, the appearance of the effective xenon cross section in this problem.

---

* R. R. Schiff, The Space Simulator Method for Solving the Group Diffusion Equations, WAPD-105, March 1954.

Section 2 of this paper is devoted to a discussion of the effective xenon cross section in the xenon override problem. Section 3 is concerned with the role of the Nordheim perturbation problem in the temperature coefficient problem. Section 4 includes a discussion of the appearance and interpretation of the effective xenon cross section in a particular temperature coefficient problem. Section 5 is devoted to a discussion of new techniques of calculating the effective xenon cross section in the xenon override problem. The paper is concluded with Section 6, which contains the results of numerical calculations associated with the techniques described in Section 5.

Two examples are studied in Section 6 which are fictitious in the sense that the rod configurations involved do not coincide exactly with actual experimental situations. However, both examples are admirably suited to illustrate the improved techniques of calculating the effective xenon cross section developed in this paper. The first example is of importance in illustrating techniques which are applicable in the case of a preshutdown configuration involving partially lifted xenon rods. The second example is of particular interest since the preshutdown configuration with all xenon rods fully inserted corresponds to the conditions assumed to prevail in all previous studies on the xenon override problem. Both cases serve to illustrate the striking effect of the preshutdown power level on the thermal flux distribution at the time of xenon override and on the over-all effective xenon cross section and reveal convincingly earlier misconceptions on the problem.

2. The Xenon Override Problem

In WAPD-RM-128 the effective xenon cross section was defined to be

$$(2.1) \qquad \left\langle \Sigma_P \right\rangle_{eff} = \Sigma_{25} \left\langle A + B\,\alpha \frac{Q}{\Sigma_{25}^f} \right\rangle,$$

where Q is the power level preceding shutdown in fissions per second, where α is called the weighting factor associated with the distribution Φ_s and is given by the formula

$$(2.2) \qquad \alpha = \frac{V_{core} \int_{core} \Phi_s \varphi_s \varphi_s^* \, dV}{\int_{core} \Phi_s \, dV \int_{core} \varphi_s \varphi_s^* \, dV},$$

and where A(t) and B(t) are functions of the xenon cross section, $\bar{\sigma}_X$, the samarium cross section, $\bar{\sigma}_S$, and various other parameters which may be considered as constants throughout this discussion. The flux Φ_s represents the xenon (or samarium) distribution at the time of shutdown, and φ_s and φ_s^* represent fluxes in the homogeneous reactor at the time of override of maximum xenon, for example, when all control rods (save half the regulator rod) are assumed to be out of the reactor.

In the use of formula (2.1), in the past, it has been tacitly assumed that the perturbation in the flux φ_s, as a result of the inhomogeneous distribution of xenon as opposed to its homogeneous distribution, is very small. Two examples have been studied recently which indicate that the perturbation under discussion may be a substantial one and that the unreserved use of formula (2.1) may lead to invalid results. Thermal flux distributions associated with these two examples are discussed in detail in Section 6.

The restriction in the conventional use of the Nordheim perturbation formula is that the perturbation in the flux, as a result of whatever disturbance in the reactor is being studied, is so small as to be negligible. The restriction arises from the replacement of the perturbed flux by the first term in its Taylor's expansion. The need for such a restriction stems from the lack of knowledge of the perturbed flux in most situations involving application of the Nordheim formula. Reference to the method of derivation of the Nordheim formula, as described in WAPD-19, indicates the adjustments which should be made to the weighting factor (2.2) for the case of large perturbations. Thus, for large perturbations (2.1) should properly be written in the form

$$\alpha = \frac{V_{core} \int_{core} \Phi_s \, \varphi_s \varphi_{s_o}^{\star} \, dV}{\int_{core} \Phi_s \, dV \int_{core} \varphi_s \varphi_{s_o}^{\star} \, dV}, \tag{2.3}$$

where the subscript zero pertains to the flux in the unperturbed reactor with all rods removed and a homogeneous distribution of xenon, and where the flux φ_s is the perturbed flux arising from the inhomogeneous distribution of xenon.

Since the perturbed flux φ_s is known, in the studies of this paper, formula (2.3) will henceforth be used in calculations of the weighting factor. Indeed, the validity of (2.1) is strongly open to question in any studies except possibly in situations where the power level preceding shutdown is very low.

Techniques of evaluating (2.3) and computing the effective xenon cross section in the xenon override problem will be discussed in Section 5 of this paper.

3. Interpretations of the Nordheim Perturbation Formula

The so-called period-inhour relationship for a bare homogeneous reactor is given by the formula*

$$(3.1) \qquad \delta\rho = \frac{\Delta k_{eff}}{k_{eff}} = \frac{\ell^*}{T\, k_{eff}} + \sum_i \frac{\beta_i T_i}{T + T_i} .$$

An analogous relationship obtained by Nordheim in the derivation of the Nordheim perturbation formula is the formula

$$(3.2) \qquad \int_{\text{reactor}} \Big\{ \delta(k\Sigma_s)\varphi^*_{f_o}\varphi_s + \delta\Sigma_f(\varphi^*_{s_o}\varphi_f - \varphi^*_{f_o}\varphi_f) - \delta\Sigma_s\varphi^*_{s_o}\varphi_s$$

$$- \delta D_s \nabla\varphi^*_{s_o} \cdot \nabla\varphi_s - \delta D_f \nabla\varphi^*_{f_o} \cdot \nabla\varphi_f \Big\}\, dV \doteq \int_{\text{core}} \Sigma_s k_p \varphi^*_{f_o}\varphi_s dV$$

$$= \frac{1}{T} \int_{\text{reactor}} \left\{ \frac{\varphi^*_{s_o}\varphi_s}{v_s} + \frac{\varphi^*_{f_o}\varphi_f}{v_f} \right\} dV \doteq \int_{\text{core}} \Sigma_s k_p \varphi^*_{f_o}\varphi_s dV + \sum_i \frac{\beta_i T}{T + T_i} ,$$

which is valid for an inhomogeneous reflected reactor. In this formula the subscript zero refers to the unperturbed flux; otherwise, the flux is the perturbed flux.

An identification between (3.1) and (3.2) is made by the summation term which is common to the two formulas. Then, by definition,

---

* The reader is referred to WAPD-19 for an explanation of the notation used in this section.

$$(3.3)\qquad \frac{\ell^{\bigstar}}{k_{eff}} = \int_{reactor} \left\{ \frac{\varphi^{\bigstar}_{s_o}\varphi_s}{v_s} + \frac{\varphi^{\bigstar}_{f_o}\varphi_s}{v_f} \right\} dV \div \int_{core} \Sigma_s k_p \varphi^{\bigstar}_{f_o} \varphi_f dV,$$

$$(3.4)\qquad \delta\rho = \int_{reactor} \Big\{ \delta(k\Sigma_s \varphi^{\bigstar}_{f_o}\varphi_s) + \delta\Sigma_f(\varphi^{\bigstar}_{s_o}\varphi_f - \varphi^{\bigstar}_{f_o}\varphi_f) - \delta\Sigma_s\varphi^{\bigstar}_{s_o}\varphi_s$$

$$- \delta D_s \nabla\varphi^{\bigstar}_{s_o} \circ \nabla\varphi_s - \delta D_f \nabla\varphi^{\bigstar}_{f_o} \cdot \nabla\varphi_f \Big\} dV \div \int_{core} \Sigma_s k_p \varphi^{\bigstar}_{f_o}\varphi_s dV.$$

Formula (3.4) affords a generalization of k_{eff} (or of reactivity), as known for a bare homogeneous reactor, to the case of a reflected inhomogeneous reactor, and formula (3.3) provides a similar generalization of the lifetime, $\ell^{\bigstar}$, in a finite reactor. These are bona fide generalizations in the sense that both formulas reduce to the conventional definitions of k_{eff} and $\ell^{\bigstar}$ for a bare homogeneous reactor, when the perturbed flux is replaced by the unperturbed flux and when the fluxes associated with a bare homogeneous reactor are used.

In the light of the preceding discussion it might be argued that formula (3.1) leads to incorrect results, for example, in connection with the calibration of control rods in a reactor so highly inhomogeneous.

Indeed, this might well be the case except that the measured periods are so large that, in (3.1), the first term is always small as compared to the second term. However, in a study of reactor accidents, where very small periods might be encountered, the use of (3.3) as a definition of the lifetime would improve markedly the accuracy of reactivity calculations.

The use of <u>generalized reactivity</u>, as given by formula (3.4), might well improve the accuracy of temperature coefficient calculations in a reactor with its complicated configurations of control rods.

While this paper is not concerned specifically with temperature coefficient calculations, the reappearance of the effective xenon cross section in the temperature coefficient problem at the time of maximum xenon override accounts for the discussion in this and the following section.

---

4. The Temperature Coefficient Problem

In the determination of the temperature coefficient at the time of override of maximum xenon, with the aid of the generalized reactivity formula, the contribution to the temperature coefficient of the term involving the xenon (plus samarium) is given by

$$(4.1) \qquad -\int_{\text{core}} \frac{\partial \Sigma_X}{\partial T} \varphi^{\ast}_{s_o} \varphi_s dV \div \int_{\text{core}} \Sigma_s k_p \varphi^{\ast}_{f_o} \varphi_s dV,$$

since the variation of the samarium cross section with temperature is essentially constant.* The xenon cross section can be written in the form

$$(4.2) \qquad \Sigma_X = \bar{\sigma}_X (C + D\, c\, \Phi_s),$$

where in this discussion C and D are independent of the temperature, where c is a normalizing factor which depends on the power level, the amount of fuel, and the operating flux preceding shutdown, and where Φ_s represents the xenon distribution. When c is properly evaluated* (4.2) becomes

$$(4.3) \qquad \Sigma_X = \bar{\sigma}_X \left(C + \frac{D\, V_{\text{core}}\, Q}{\Sigma^f_{25} \int_{\text{core}} \Phi_s dV} \Phi_s \right),$$

where Q is the power level preceding shutdown measured in fissions per second.

---

* Cf. WAPD-RM-128.

Substitution of (4.3) into (4.1) gives

$$-\frac{\partial(\Sigma_X)_{eff}}{\partial T}\int_{core}\varphi^{\star}_{s_o}\varphi_s dV \div \int_{core}\Sigma_s k_p \varphi^{\star}_{f_o}\varphi_s dV, \tag{4.4}$$

where

$$(\Sigma_X)_{eff} = \bar{\sigma}_X \left[C + \alpha D \frac{Q}{\Sigma^f_{25}} \right], \tag{4.5}$$

and

$$\alpha = \frac{V_{core}\int_{core}\Phi_s \varphi^{\star}_{s_o}\varphi_s \, dV}{\int_{core}\Phi_s \, dV \int_{core}\varphi^{\star}_{s_o}\varphi_s \, dV}. \tag{4.6}$$

From the aspect of <u>form</u>, (4.5) and (4.6) can now be identified with (2.1) and (2.3), respectively. However, the interpretations of the weighting factors (2.3) and (4.6) are quite different. In the first place, the perturbation in the flux as a result of a unit change in temperature is indeed a small perturbation. Thus, the subscript zero in (4.6) can be dropped and the flux φ_s taken as the unperturbed flux. In the situation at hand, the unperturbed flux φ_s is the thermal flux at the time of xenon override with shim and xenon rods fully withdrawn. Typical examples of such a flux are the distributions pictured in Section 6. Thus, the xenon weighting factor, α, in the xenon override problem and in the temperature coefficient problem at the time of xenon override have quite different interpretations.

5. Techniques of Evaluating the Effective Xenon Cross Section

The technique of evaluating the weighting factor ω in the xenon override problem of WAPD-RM-128 implies the writing of (2.3) in the separable form $\omega = \alpha_r \alpha_z$, where

$$(5.1) \qquad \alpha_r = \frac{\int_0^a r\,dr \int_0^a r\,\bar{\Phi}_s^{\theta}(r)\varphi_{s_o}^{\star}(r)\varphi_s(r)dr}{\int_0^a r\,\bar{\Phi}_s^{\theta}(r)dr \int_0^a r\,\varphi_{s_o}^{\star}(r)\varphi_s(r)dr},$$

$$(5.2) \qquad \alpha_z = \frac{\int_0^h dz \int_0^h \Phi_s(z)\varphi_{s_o}^{\star}(z)\varphi_s(z)dz}{\int_0^h \Phi_s(z)dz \int_0^h \varphi_{s_o}^{\star}(z)\varphi_s(z)dz},$$

and where a and h are the radius and the altitude of the core, respectively. This procedure implies not only the separability of the xenon distribution function Φ_s but also the separability of the fluxes $\varphi_{s_o}^{\star}$ and φ_s. It is also recalled that in WAPD-RM-128 an effort was made to compute the number α_r as accurately as possible on the basis of many laboriously calculated Nordheim-Scalettar distributions, and further that α_z was calculated on the basis of cosine distributions for all of the axial distributions involved in (5.2)

The assumption of separability of the xenon distribution function Φ_s seems to be a reasonable one, at least on the basis of currently available techniques for the calculation of flux distributions. It is an assumption which is invalid only by virtue of the geometric inhomogeneities introduced by the control rods and the reflector. However, the assumption of separability of the functions $\varphi_{s_o}^{\star}$ and φ_s is weakened not only by the geometric inhomogeneities but also by the inhomogeneous distribution of the xenon.

In the discussion which follows the assumption of separability of the xenon distribution function Φ_s will persist, but on the basis of the ideas which have been partially advanced in Section 2 it can no longer be assumed that $\varphi^*_{s_o}$ and φ_s are separable, at least in the usual sense. An immediate implication of this conclusion is that the weighting function α cannot be assumed to be separable into the component parts α_r and α_z. These remarks will be clarified later in the discussion.

Since the xenon distribution Φ_s is assumed to be separable, it can be written in the form*

$$\Phi(r,\theta,z) = c\mathcal{R}(r,\theta)\mathcal{Z}(z), \tag{5.3}$$

where c depends on the power level preceding shutdown. Examples of the distribution $\mathcal{Z}(z)$ are given by the distributions displayed in Section 6. The distribution $\mathcal{R}(r,\theta)$ has been approximated by various methods at the Westinghouse Atomic Power Division: (i) the Nordheim-Scalettar technique of WAPD-RM-128, (ii) the two-dimensional analogue machines, (iii) the one-dimensional analogue machine (the GODDESS), where the control rod rings are simulated by annuli.

To determine the parameter c in (5.3), first let it be supposed that $c\mathcal{R}(r,\theta) \equiv d$, where d is a constant and where it is understood that, in the determination of $\mathcal{Z}(z)$, the radial buckling is contained in the absorption constants. Then, if Q is measured in fissions per second,

---

* Since all fluxes under discussion in this section are thermal, the subscript s will henceforth be omitted. The changes in notation which are made are self-explanatory.

$$Q = \int_V \Phi(r,\theta,z)\Sigma_{25}^f \, dV$$

$$= \pi a^2 \Sigma_{25}^f \, d \int_0^h \mathcal{Z}(z) dz$$

$$= V\Sigma_{25}^f \, d \, \overline{\mathcal{Z}}(z),$$

whence

$$d = \frac{Q}{V\Sigma_{25}^f \overline{\mathcal{Z}}(z)} .$$

Then, define

$$\Phi(z) = \frac{Q}{V\Sigma_{25}^f} \frac{\mathcal{Z}(z)}{\overline{\mathcal{Z}}(z)} . \tag{5.4}$$

Now, in a plane $z = z_o$, the average flux over r and θ is given by (5.4). Thus,

$$\overline{\Phi}^{r,\theta}(r,\theta,z_o) = c\mathcal{Z}(z_o) \frac{\int_S \mathcal{R}(r,\theta) r dr d\theta}{\int_S r dr d\theta} = \frac{Q}{V\Sigma_{25}^f} \frac{\mathcal{Z}(z_o)}{\overline{\mathcal{Z}}(z)},$$

whence

$$c = \frac{Q}{V\Sigma_{25}^f \overline{\mathcal{R}}(r,\theta) \overline{\mathcal{Z}}(z)} . \tag{5.5}$$

The point of view in the development which follows is influenced greatly by the geometric fact that the rods are capable of moving axially but not radially. Thus, it is convenient at the outset to define a radial weighting factor $\alpha_r(z_o)$ in a plane $z = z_o$, and then consider a summation process over z to obtain finally an over-all weighting factor ω. In any plane $z = z_o$ the maximum xenon cross section is of the form

$$(5.6) \qquad (\Sigma_X)_{max} = A + B\Phi(r,\theta,z_o)$$

$$= A + B \frac{\Phi(z_o)}{\overline{\mathcal{R}}(r,\theta)} \mathcal{R}(r,\theta).$$

The corresponding effective xenon cross section is given by

$$(5.7) \qquad (\Sigma_X)_{eff} = A + B\, \alpha_{r,\theta}(z_o)\Phi(z_o),$$

where $\Phi(z_o)$ is obtained from (5.4).

It is interesting at this juncture to consider the structure of the perturbed flux $\varphi(r,\theta,z)$ at the time of maximum xenon override. Suppose for the moment, as a matter of convenience, that φ is independent of θ. The perturbed flux φ in any plane $z = z_o$ is certainly influenced by the xenon distribution (5.6) in that plane. Thus, the radial component of φ in the plane $z = z_o$ is of the form $R = R[r, \Phi(r,z_o)]$. In principle, this function must be known before the weighting factor $\alpha_r(z_o)$ can be determined. Indeed, the radial weighting factor can be written in the form

$$(5.8) \qquad \alpha_r(z_o) = \frac{\int_0^a r\, dr}{\int_0^a \Phi(r,z_o) r dr} \cdot \frac{\int_0^a \Phi(r,z_o) R[r,\Phi(r,z_o)] R^*[r,\Phi(r,z_o)] r\, dr}{\int_0^a R[r,\Phi(r,z_o)] R^*[r,\Phi(r,z_o)] r\, dr}.$$

The axial component of $\varphi(r,z)$ cannot be found until $\alpha_r(z)$, and consequently $[\bar{\Sigma}_X(z)]_{eff}$, is known. Thus, the total perturbed flux is of the form

$$\varphi(r,z) = R[r,\Phi(r,z)]\ Z\ [\alpha_r(z)], \tag{5.9}$$

where it is noted that Z is a function of z alone. Although $\varphi(r,z)$ is not separable, as indicated above, the form of (5.9) suggests that $\varphi(r,z)$ might appropriately be termed quasi-separable.

When an analogue machine, such as the GODDESS, is available for calculations, the radial weighting factor $\alpha_r(z)$ can be determined by a much simpler technique than the direct evaluation of the formula (5.8). Since η is the variable parameter to be determined for criticality in the use of the GODDESS, then η can be determined as a function of Σ_{eff} in the relation (5.7), as indicated in Figure 5.1. This follows since the homogeneous poison parameter $\Sigma_{eff}(z_o)$ is a function of z_o in each homogeneous criticality calculation in a plane $z = z_o$. Consequently, η varies with z_o, and hence $\Sigma_{eff}(z_o)$ varies with η. Moreover, the parameter $\Sigma_{max}(z_o)$ is a function of $\Phi(z_o)$ in each heterogeneous reactor calculation in a plane $z = z_o$. Thus, η varies with z_o and consequently with $\Phi(z_o)$, where the relationship between η and $\Phi(z_o)$ is also displayed in Figure 5.1.

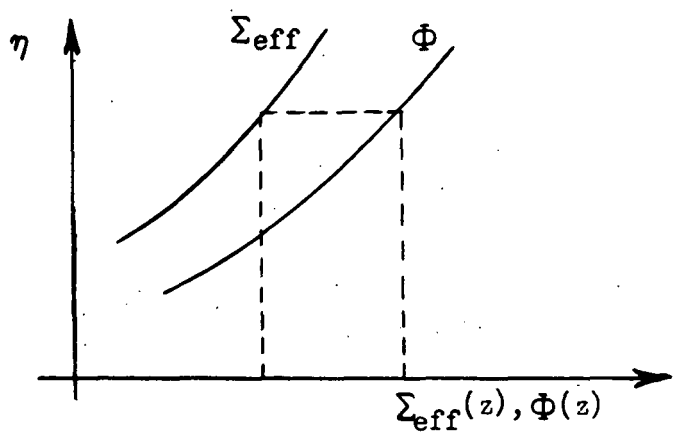

Figure 5.1

A correspondence between $\Sigma_{eff}(z)$ and $\Phi(z)$ is now established by the matching of η's in Figure 5.1. Finally, from formula (5.7), $\alpha_{r,\theta}(z)$ is determined. In this connection, it must be noted that $\alpha_{r,\theta}(z)$ is a continuous function of z only in the situation that the xenon rods are fully inserted and the shim rods are fully withdrawn preceding shutdown. If a bank of three or six xenon rods are lifted during operation at full power with equilibrium xenon, then two axial regions (neglecting the regulator rod) are generated. Then, $\mathcal{R}(r,\theta)$ differs in each of the two axial regions, thus creating a discontinuity in $\alpha_{r,\theta}(z)$. Such a discontinuity, however, does not present a serious mathematical obstacle.

The next step in the mathematical analysis of this discussion is to find the over-all or total weighting factor ω and consequently the over-all effective maximum xenon cross section. In this connection, the radial effective xenon cross section, given by (5.7), becomes the over-all maximum xenon cross section. Thus,

$$(5.10) \qquad \left[\Sigma_X(z)\right]_{max} = A + B\,\alpha_{r,\theta}(z)\Phi(z),$$

and it is desired to find

$$(5.11) \qquad (\Sigma_X)_{eff} = A + B\,\omega\bar{\Phi},$$

where

$$(5.12) \qquad \bar{\Phi} = \frac{1}{h}\int_0^h \Phi(z)dz = \frac{Q}{V\Sigma_{25}^f h}\int_0^h \frac{\mathcal{Z}(z)}{\mathcal{Z}(z)}\,dz = \frac{Q}{V\Sigma_{25}^f}.$$

From the definition of effective maximum xenon cross section it follows that

$$(5.13)\qquad \int_o^h \left[\Sigma_X(z)\right]_{max} Z(z)Z_o^*(z)dz = \int_o^h (\Sigma_X)_{eff} Z(z)Z_o^*(z)dz,$$

where $Z\left[\alpha_{r,\theta}(z)\right] = Z(z)$. Substitution of the expressions (5.10) and (5.11), for the xenon cross sections, into (5.13) yields the result

$$(5.14)\qquad \omega = \frac{\int_o^h dz \int_o^h \alpha_r(z)\,\Phi(z)Z(z)Z_o^*(z)dz}{\int_o^h \Phi(z)dz \int_o^h Z(z)Z_o^*(z)dz}.$$

Note that if $\alpha_r(z)$ were constant throughout the core, the total weighting factor could be written in the separable form $\omega = \alpha_r\alpha_z$, where α_z is given by (5.2).

In Section 6, comparisons are made between the use of (5.14), with a variable radial weighting factor, and the use of the separable form $\omega = \alpha_r\alpha_z$, with a constant radial weighting factor.

6. Results of Numerical Calculations

This section is devoted to the evaluation of the effective xenon cross sections, associated with two different preshutdown rod configurations, with the use of the techniques outlined in the preceding section. The two cases studied are described as follows.

Case I. Preshutdown Configuration with Group IIIA Rods Partially Lifted

Calculation -- Xenon Override

Initial State

Rods	Position (inches)
Group I	43
Group II	43
Group IIIA	10.95
Group IIIB	0

Reactor Poisons: equilibrium poisons at full power

Loading: no depletion

Final State

Rods	Position (inches)
Group I	43
Group II	43
Group IIIA	43
Group IIIB	43

Reactor Poisons: maximum xenon

Loading: same as in initial state

Actual Experiment -- Xenon Override

Initial State

Rods	Position (inches)
Group I	37.2
Group II	37.2
Group IIIA	11.8
Group IIIB	0

Reactor Poisons: equilibrium poisons at full power

Loading: after 93 hours at full power, 19.86 kg

Date of Experiment: June 25 to 29, 1953

Final State

Rods	Position (inches)
Group I	37.3
Group II	37.3
Group IIIA	37.9
Group IIIB	23.6

Reactor Poisons: maximum xenon

Loading: same as in initial state

Case II. Preshutdown Configuration with Xenon Rods Fully Inserted

Calculation -- Xenon Override

Initial State

Rods	Position
Group I	out
Group II	out
Group IIIA	in
Group IIIB	in

Reactor Poisons: equilibrium poisons at full power

Loading: no depletion

Final State

Rods	Position
Group I	out
Group II	out
Group IIIA	out
Group IIIB	out

Reactor Poisons: maximum xenon

Loading: same as in initial state

It is evident, from examination of the conditions pertaining to the actual xenon override experiment, described under Case I, that both theoretical problems studied in this paper are purely fictitious. However, the principal object of this paper is to exhibit improved techniques of calculating the effective xenon cross section, and the problems studied yield results which are highly instructive. Case I is of importance in illustrating techniques which are applicable in the case of a preshutdown configuration involving partially lifted xenon rods. Case II is of particular interest, since the preshutdown configuration of all shim rods out and all xenon rods in corresponds to the conditions assumed to prevail in all previous studies on the xenon override problem. Both cases serve to illustrate the striking effect of the preshutdown power level on the thermal flux distribution at the time of maximum xenon override and on the over-all effective xenon cross section. The calculations are explained in detail in the step-wise procedure which follows.

Case I

Preshutdown Configuration with Group IIIA Rods Partially Lifted

Step 1. Preshutdown Radial Flux Distribution

The reactor used in this calculation was considered as undepleted with equilibrium xenon at 460°F. The xenon bank was considered as fully inserted and represented by an annulus of rod material. The shim bank was considered as fully withdrawn and the resulting lacunae represented by a water annulus. The regulator rod was considered as fully withdrawn and the resulting lacuna represented by a circular water hole. Flux distributions were found for this reactor.

Step 2. Xenon Override with Uniform Poison (Radial Case)

The xenon rods are fully withdrawn. In any horizontal cross section a uniform poison $(\Sigma_X)_{eff}$ is given by (5.7), that is,

$$(6.1) \qquad (\Sigma_X)_{eff} = A + B\, \alpha_r(z_o)\Phi(z_o),$$

where

$$(6.2) \qquad A = .03388\ \Sigma_{25},$$

$$(6.3) \qquad B = .2052 \times 10^{-4}\ \Sigma_{25},$$

and where

$$(6.4) \qquad \Phi(z_o) = \frac{Q}{V\Sigma^f_{25}} \frac{\mathcal{Z}(z_o)}{\overline{\mathcal{Z}}(z)}$$

is the preshutdown flux averaged over the plane $z = z_o$.

Any given value of $\alpha_r(z_o)\Phi(z_o)$ leads to a particular value of $[\Sigma_X(z_o)]_{eff}$ which is constant throughout the plane $z = z_o$. By use of the simulator the value of η corresponding to some $(\Sigma_X)_{eff}$ can be found. Hence, it is possible to plot η as a function of $\alpha_r\Phi$. This relationship is found to be linear:

$$(6.5) \qquad \eta_r(\text{uniform}) = 1.707 + .2520 \times 10^{-14}\ \alpha_r\Phi\ .$$

The function η_r(uniform) is plotted as a function of $\alpha_r\Phi$ in Figure 6.1.

FIGURE 6.1

η VERSUS $\alpha_r \Phi$ AND Φ

RADIAL CASE (Refer to Case I, Steps 2 and 3)

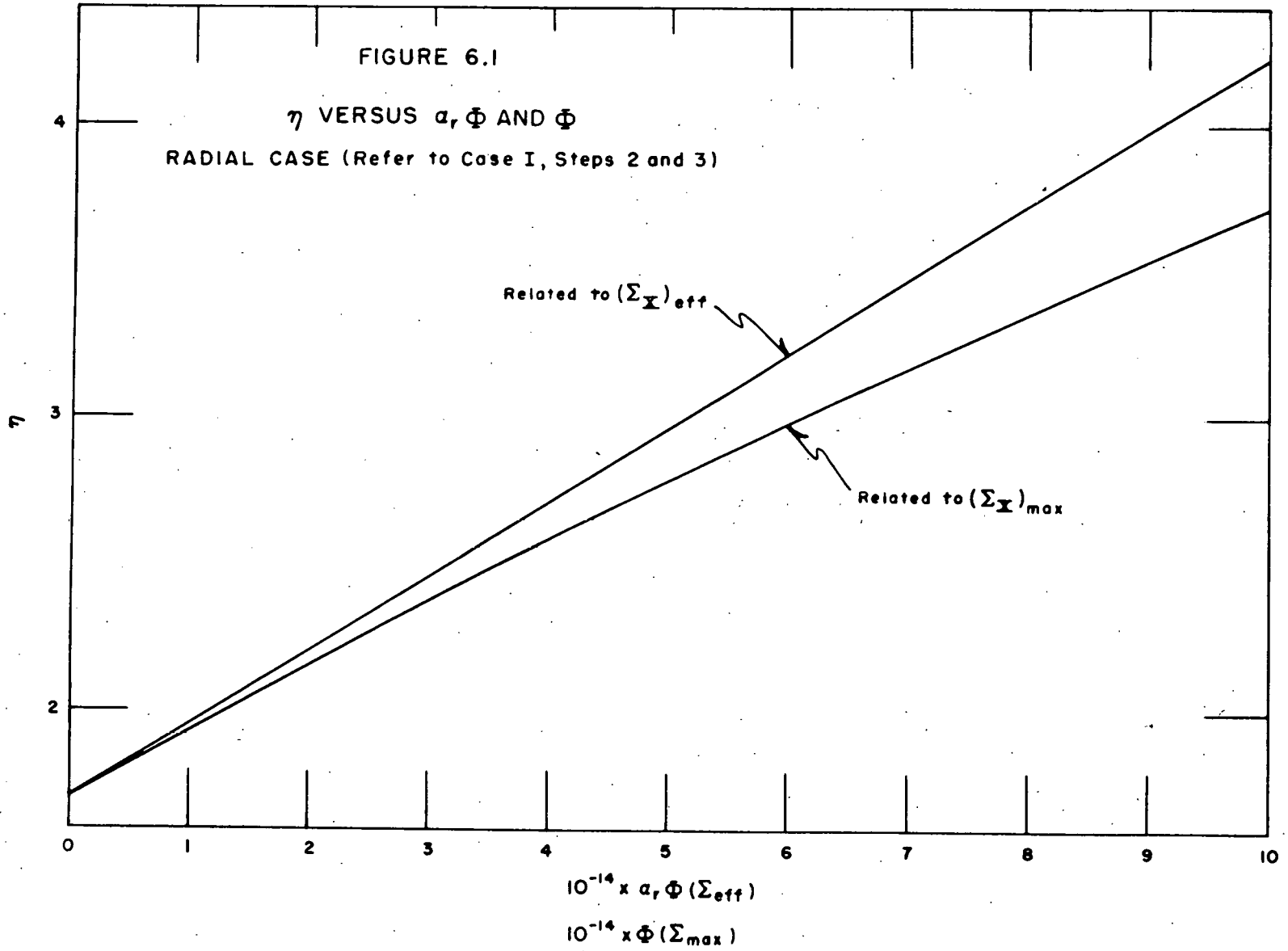

Step 3. Xenon Override with Non-Uniform Poison (Radial Case)

The maximum xenon cross section in a plane $z = z_o$ is given by (5.6), that is,

$$(\Sigma_X)_{max} = A + B \frac{\Phi(z_o)}{\mathcal{R}(r)} \mathcal{R}(r). \tag{6.6}$$

When the simulator is used to solve the criticality problem in a plane $z = z_o$, with the non-uniform poison distribution given by (6.6), η_r(non-uniform) is obtained as a function of Φ. This relationship, which is non-linear, is also plotted in Figure 6.1.

The matching of η's in Figure 6.1 generates a functional relationship between α_r and Φ which is displayed in Figure 6.2. The procedure described in Steps 1 and 2 is the equivalent of that described in Section 5 in connection with the schematic diagram of Figure 5.1.

Step 4. Preshutdown Axial Flux Distribution

The problem considered from a radial point of view in the preceding steps is now continued from an axial point of view. The configuration under consideration is pictured from a schematic point of view in Figure 6.3. In this configuration $\Sigma_{P_o} = .010\ cm^{-1}$ was assigned to all of the xenon rods, and the poison worth of the IIIA bank of xenon rods in region II was found to be $\Sigma_P = .006\ cm^{-1}$ corresponding to criticality ($\eta = 2.12$). Flux distributions are available for this configuration, the thermal flux being pictured in Figure 6.5.

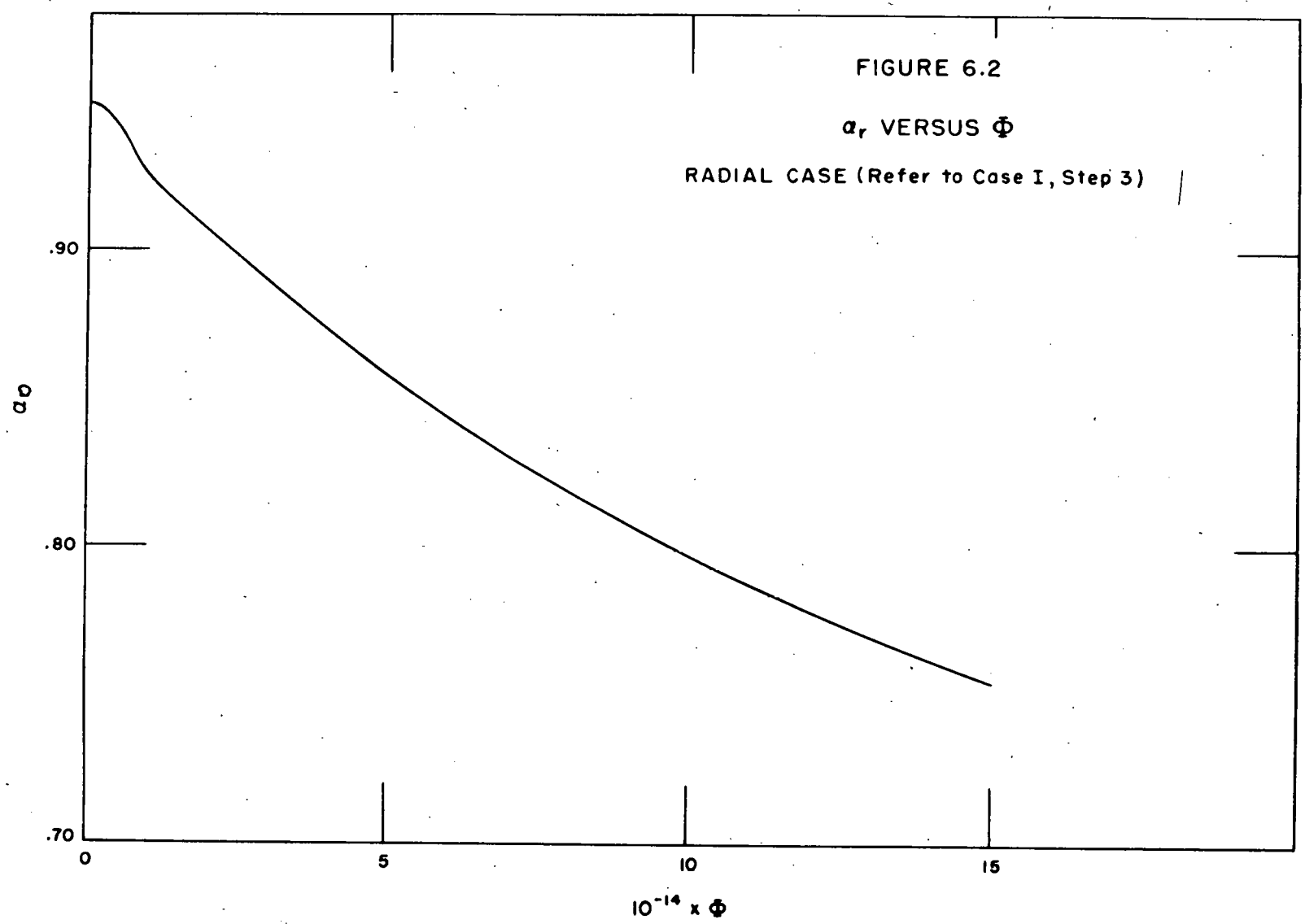

FIGURE 6.2

α_r VERSUS Φ

RADIAL CASE (Refer to Case I, Step 3)

460°F with Equilibrium Poisons

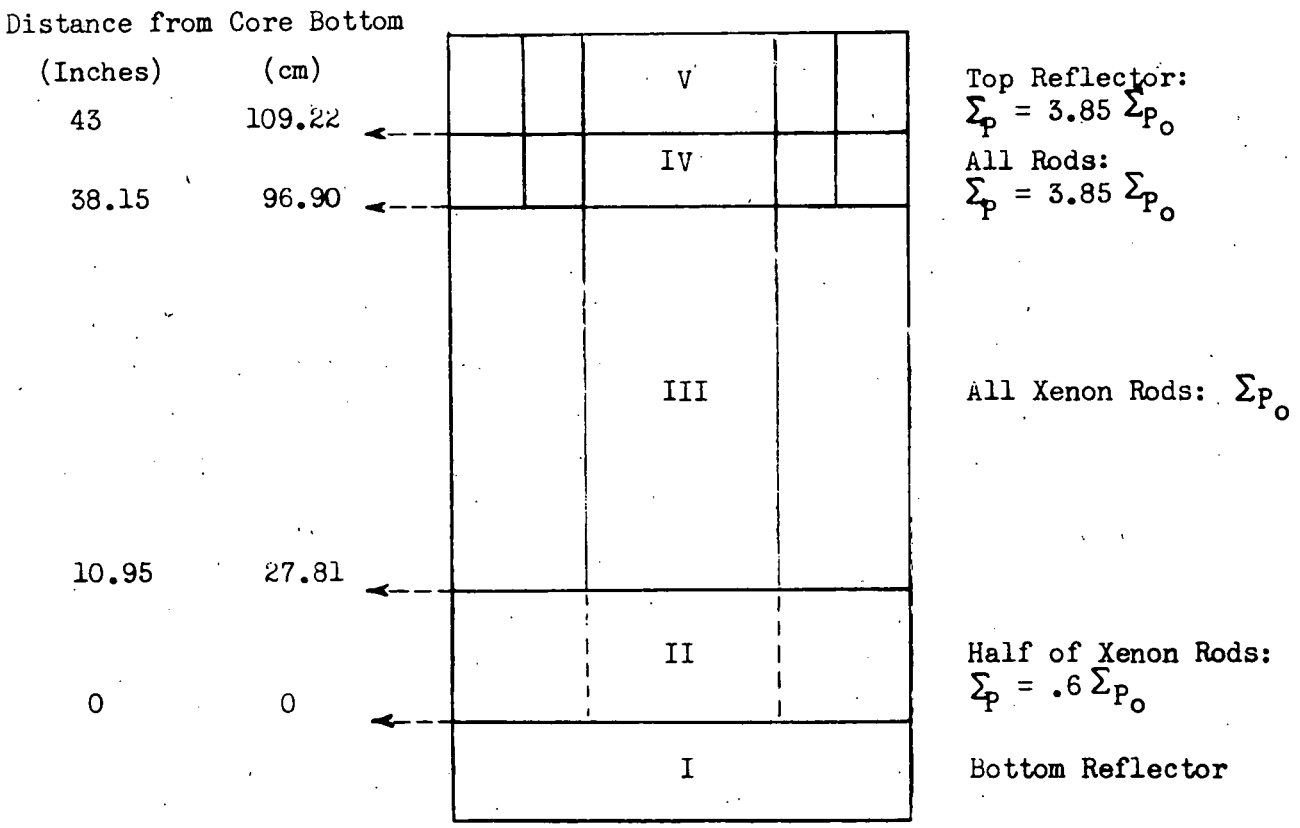

Figure 6.3

Step 5. Xenon Override with Uniform Poison (Axial Case)

The xenon rods are withdrawn and consideration is given to an over-all $(\Sigma_X)_{eff}$. In this connection, equation (5.11) is

$$(6.7) \qquad (\Sigma_X)_{eff} = A + B\,\omega\,\bar{\Phi},$$

where ω is the over-all weighting factor, and where

$$(6.8) \qquad \bar{\Phi} = \frac{1}{h}\int_o^h \Phi(z)dz = \frac{Q}{V\Sigma_{25}^f h}\int_o^h \frac{\mathcal{Z}(z)}{\overline{\mathcal{Z}}(z)}\,dz = \frac{Q}{V\Sigma_{25}^f}.$$

As in Step 2, plot η versus $\omega\bar{\Phi}$. This relationship is found to be linear and is given by

$$\eta(\text{uniform}) = 1.686 + .2532 \times 10^{-14}\, \omega\bar{\Phi}. \tag{6.9}$$

Step 6. Xenon Override with Non-Uniform Poison (Axial Case)

The reactor must now be considered from a one-dimensional axial point of view. In any horizontal cross section the non-uniform xenon distribution is replaced by the radial effective xenon cross section (5.7). In the axial problem the radial effective xenon cross section becomes the over-all maximum xenon cross section. Thus, as in (5.10),

$$\left[\bar{\Sigma}_X(z)\right]_{max} = A + B\, \alpha_r(z)\Phi(z), \tag{6.10}$$

where

$$\Phi(z) = \frac{Q}{v\Sigma_{25}^f}\,\frac{\mathcal{Z}(z)}{\bar{\mathcal{Z}}(z)} = \frac{\mathcal{Z}(z)}{\bar{\mathcal{Z}}(z)}\,\bar{\Phi}. \tag{6.11}$$

For a given $\bar{\Phi}$, the value of $\Phi(z)$ corresponding to any z can be found from the distribution $\mathcal{Z}(z)$ and the relation (6.11). Moreover, α_r is related to Φ in Figure 6.2. Thus, for any given value of $\bar{\Phi}$, $\left[\bar{\Sigma}_X(z)\right]_{max}$ is known as a function of z. Finally, values of η associated with $\left[\bar{\Sigma}_X(z)\right]_{max}$ can be found with the aid of the one-dimensional simulator. In other words, η(non-uniform) is obtained as a function of $\bar{\Phi}$.

If η(uniform) versus $\omega\bar{\Phi}$ and η(non-uniform) versus $\bar{\Phi}$ are plotted on the same system of coordinate axes, then by matching η's, as in Step 3, ω is obtained as a function of $\bar{\Phi}$. This plot is given in Figure 6.4.

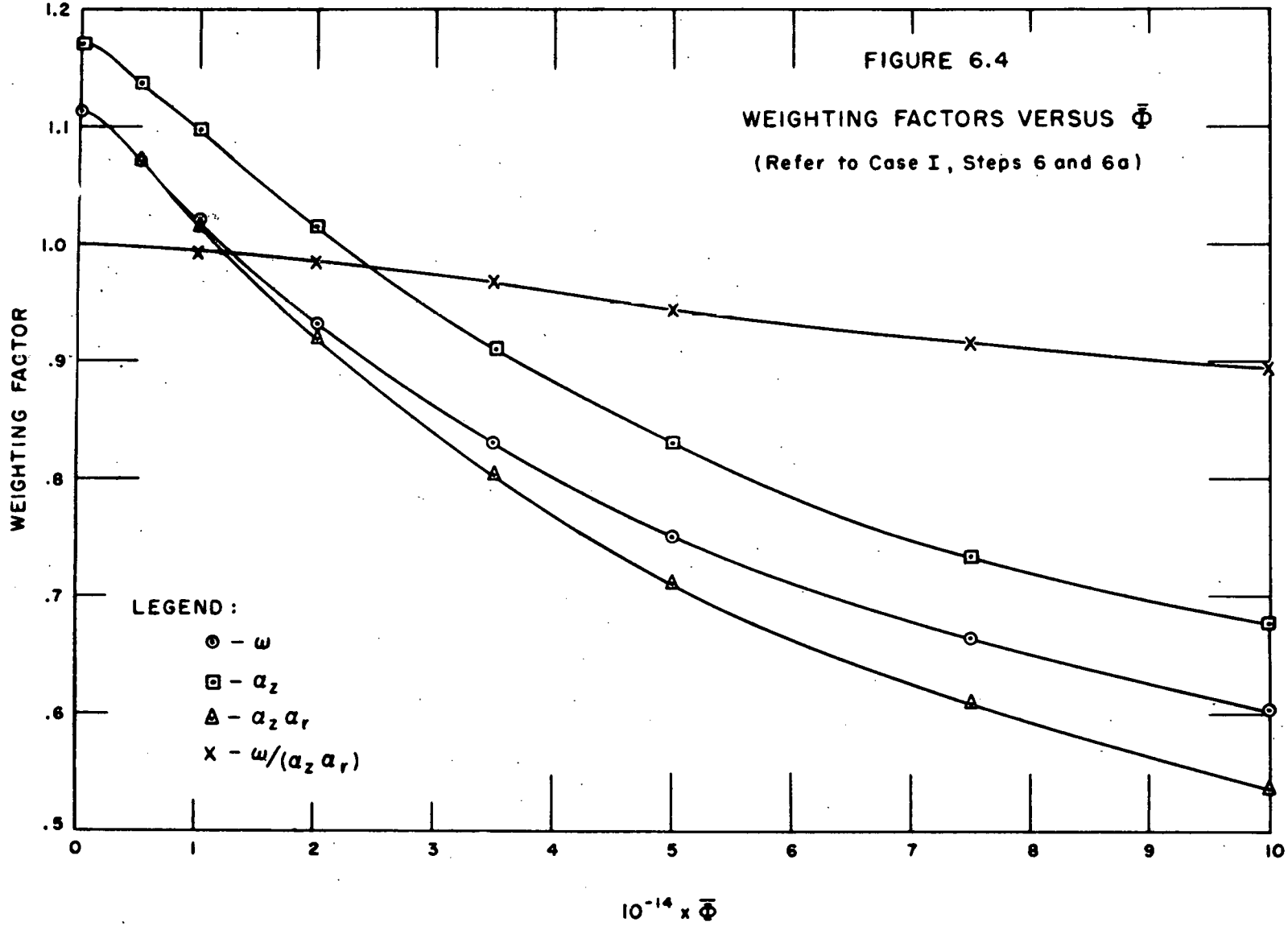
FIGURE 6.4
WEIGHTING FACTORS VERSUS $\bar{\Phi}$
(Refer to Case I, Steps 6 and 6a)
WEIGHTING FACTOR
1.2
1.1
1.0
.9
.8
.7
.6
.5
LEGEND :
⊙ – ω
⊡ – α_z
△ – $\alpha_z \alpha_r$
X – $\omega/(\alpha_z \alpha_r)$
0
1
2
3
4
5
6
7
8
9
10
$10^{-14} \times \bar{\Phi}$

Step 6a. Note that ω is the over-all weighting factor associated with tne non-separability of the axial and radial weighting factors. Previously, the axial and radial weighting factors were obtained separately and the over-all weighting factor was written as $\alpha_r\alpha_z$. It is of interest then to compare $\alpha_r\alpha_z$ with ω.

To find $\alpha_r\alpha_z$ suppose first that α_r is unity for all z, and then proceed as in Step 6. The distribution $\overline{\Sigma_X(z)}_{max}$, corresponding to a given $\bar{\Phi}$, will not be the same as it was previously. Again, η(uniform) can be found as a function of $\alpha_z\bar{\Phi}$:

$$\eta(\text{uniform}) = 1.686 + .2532 \times 10^{-14}\, \alpha_z\bar{\Phi}, \tag{6.12}$$

and η(non-uniform), associated with $\overline{\Sigma_X(z)}_{max}$, can be found as a function of $\bar{\Phi}$. The matching of η's, as in Step 6, gives α_z as a function of $\bar{\Phi}$.

To each number $\bar{\Phi}$ there now corresponds the quantities ω, α_r, and α_z. Figure 6.4 includes plots of $\alpha_r\alpha_z$ versus $\bar{\Phi}$ and $\omega/(\alpha_r\alpha_z)$ versus $\bar{\Phi}$. The last curve is a measure of the effect of non-separability of the axial and radial weighting factors.

Figure 6.5 exhibits the preshutdown axial thermal flux, $\mathcal{Z}(z)$, and illustrates the pronounced effect of the power level on the axial thermal flux, Z(z), at the time of maximum xenon override.

Comments on Case I

1. The radial weighting factor α_r is calculated only for the case of all xenon rods inserted before shutdown and all rods out during override. This situation does not actually pertain in the problem under discussion, since the Group IIIA rods are partially raised preceding shutdown. Thus, the problem solved serves primarily to illustrate the new procedures and techniques established in this paper.

FIGURE 6.5

THERMAL FLUX DISTRIBUTIONS FOR CASE I

(Fluxes Normalized so That Average Flux Is Unity)

Xenon Override Flux Distributions
For Various Power Levels

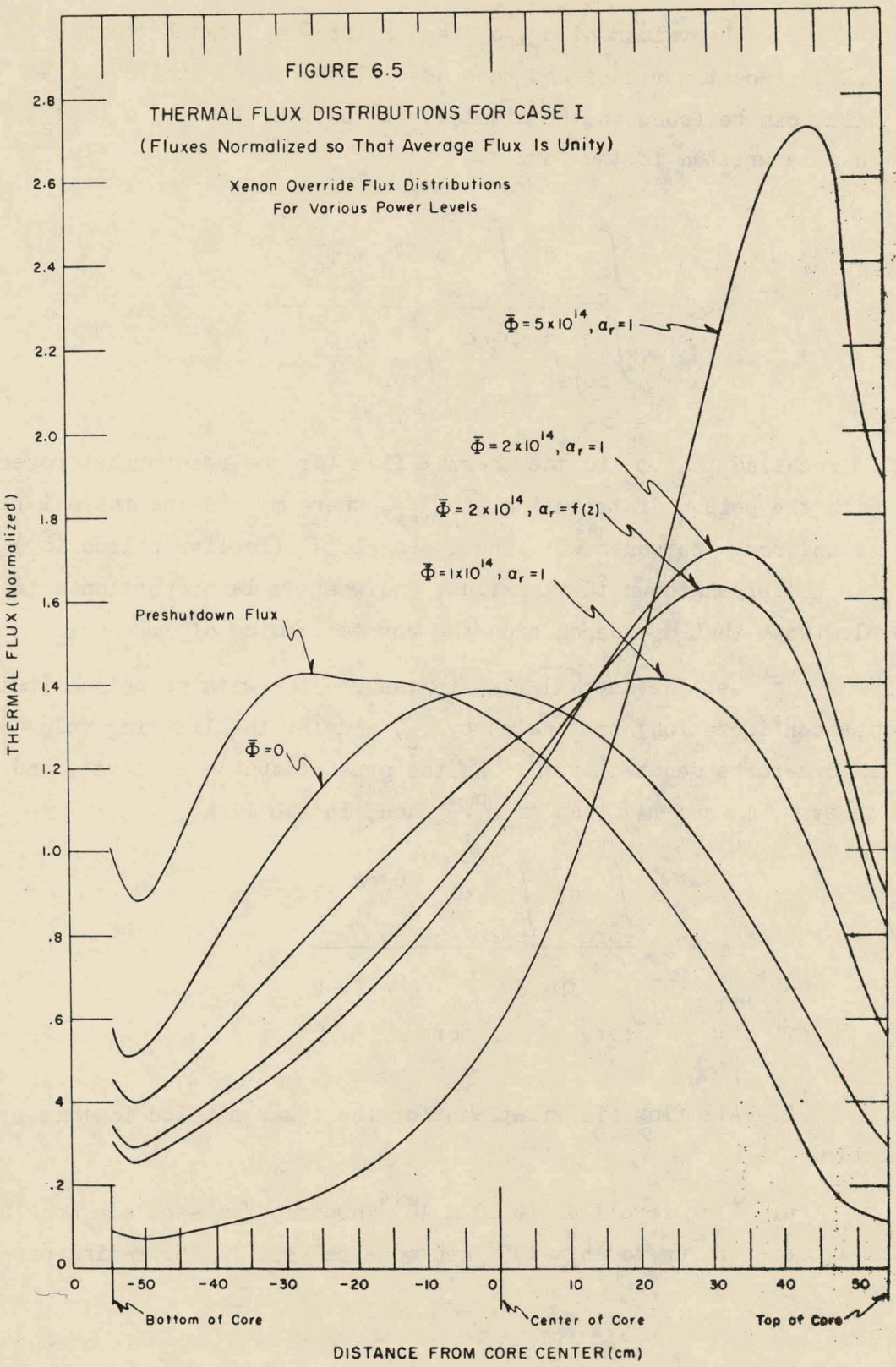

2. The values of α_r, α_z, and ω for $\bar{\Phi} = 0$ can be computed from forumla (2.3), since the fluxes and then adjoints approach limits, as $\bar{\Phi}$ tends to zero, which can be found on the simulator by setting $(\Sigma_X)_{max} = (\Sigma_X)_{eff} = 0$. Indeed, ω can be written in the form

$$\omega = \frac{\int_{core} dV \int_{core} c\, \Phi_s\, \varphi_s \varphi_{s_o}^{\dagger}\, dV}{\int_{core} c\, \Phi_s\, dV \int_{core} \varphi_s \varphi_{s_o}^{\dagger}\, dV}, \tag{6.13}$$

where it is recalled that φ_s is the thermal flux for the reactor heterogeneously poisoned with the poison distribution $(\Sigma_X)_{max}$, where φ_{s_o} is the thermal flux in the reactor uniformly poisoned with the appropriate effective poison $(\Sigma_X)_{eff}$, where Φ_s is the preshutdown thermal flux, and where c is proportional to the power level. Note that φ_{s_o} depends on the correct choice of ω.

Let the thermal flux in the reactor with no poison (but in the override configuration) be denoted by φ_s^o, and let the limiting value of ω as c tends to zero be denoted by ω^o. As the preshutdown power level, and hence c, tends to zero, φ_s and φ_{s_o} tend to φ_s^o. Then, in the limit,

$$\omega^o = \frac{\int_{core} dV \int_{core} \Phi_s\, \varphi_s^o \varphi_s^{o\dagger}\, dV}{\int_{core} \Phi_s\, dV \int_{core} \varphi_s^o \varphi_s^{o\dagger}\, dV}. \tag{6.14}$$

3. All flux distributions for the cases studied in this problem are available.

4. Flux levels up to 10×10^{14} neutrons/cm^2-sec are considered in the axial cases and up to 15×10^{14} neutrons/cm^2-sec in the radial cases.

As noted previously Case II is primarily of academic interest, since the preshutdown configuration of all shim rods withdrawn and all xenon rods fully inserted is purely fictitious with respect to the xenon override problem.

Nevertheless, consideration of the problem is of importance since the configuration studied is associated with all previous studies at the Westinghouse Atomic Power Division on the xenon override problem and since the results of the study reveal convincingly earlier misconceptions on the problem. Since qualitative results are of primary interest in Case II, the study of this case has been made for the special case in which $\alpha_r = 1$. Accordingly, the steps corresponding to Steps 1, 2, and 3 of Case I are omitted in the detailed discussion of Case II which follows.

Case II

Preshutdown Configuration with Xenon Rods Fully Inserted

Steps 1, 2, 3. These steps are omitted since $\alpha_r = 1$.

Step 4. Preshutdown Axial Flux Distribution

Since the shim rods are fully withdrawn and the xenon rods are fully inserted (the regulator rod is omitted from consideration), the axial thermal flux is a cosine in character, that is, the flux is a cosine except for the effect of the end water reflectors. This flux distribution is pictured in Figure 6.8.

Step 5. Xenon Override with Uniform Poison (Axial Case)

The over-all effective xenon cross section is of the form

$$(\Sigma_X)_{eff} = A + B\,\alpha_z \bar{\Phi} , \tag{6.15}$$

where α_z is now the over-all weighting factor, where

$$(6.16) \qquad \bar{\Phi} = \frac{1}{h}\int_0^h \Phi(z)dz = \frac{Q}{V\Sigma_{25}^f h}\int_0^h \frac{\chi(z)}{\bar{\chi}(z)}dz = \frac{Q}{V\Sigma_{25}^f},$$

and where $\chi(z)$ is the preshutdown thermal axial flux. With the aid of the simulator and the use of (6.15), η can be found as a function of $\alpha_z\bar{\Phi}$. This relationship is found to be linear, as in Case I, and is given by

$$(6.17) \qquad \eta(\text{uniform}) = 1.683 + .2532 \times 10^{-14}\,\alpha_z\bar{\Phi}.$$

Step 6. Xenon Override with Non-Uniform Poison (Axial Case)

When $\alpha_r = 1$ the over-all maximum xenon cross section is of the form

$$(6.18) \qquad \left[\bar{\Sigma}_X(z)\right]_{max} = A + B\,\Phi(z),$$

where

$$(6.19) \qquad \Phi(z) = \frac{Q}{V\Sigma_{25}^f}\,\frac{\chi(z)}{\bar{\chi}(z)} = \frac{\chi(z)}{\bar{\chi}(z)}\bar{\Phi}.$$

For a given $\bar{\Phi}$, the value $\Phi(z)$ corresponding to any z can be found from the distribution $\chi(z)$ and the relation (6.19). Then, for any given value of $\bar{\Phi}$, $\left[\bar{\Sigma}_X(z)\right]_{max}$ is known as a function of z. Finally, η(non-uniform) can be found as a function of $\bar{\Phi}$, with the use of $\left[\bar{\Sigma}_X(z)\right]_{max}$ in the simulator criticality calculations.

The relationships η(uniform) versus $\alpha_z\bar{\Phi}$ and η(non-uniform) versus $\bar{\Phi}$ are plotted on the same system of coordinate axes in Figure 6.6. The matching

FIGURE 6.6

η VERSUS $\alpha_z \bar{\Phi}$ AND $\bar{\Phi}$

AXIAL CASE (Refer to Case II, Steps 5 and 6)

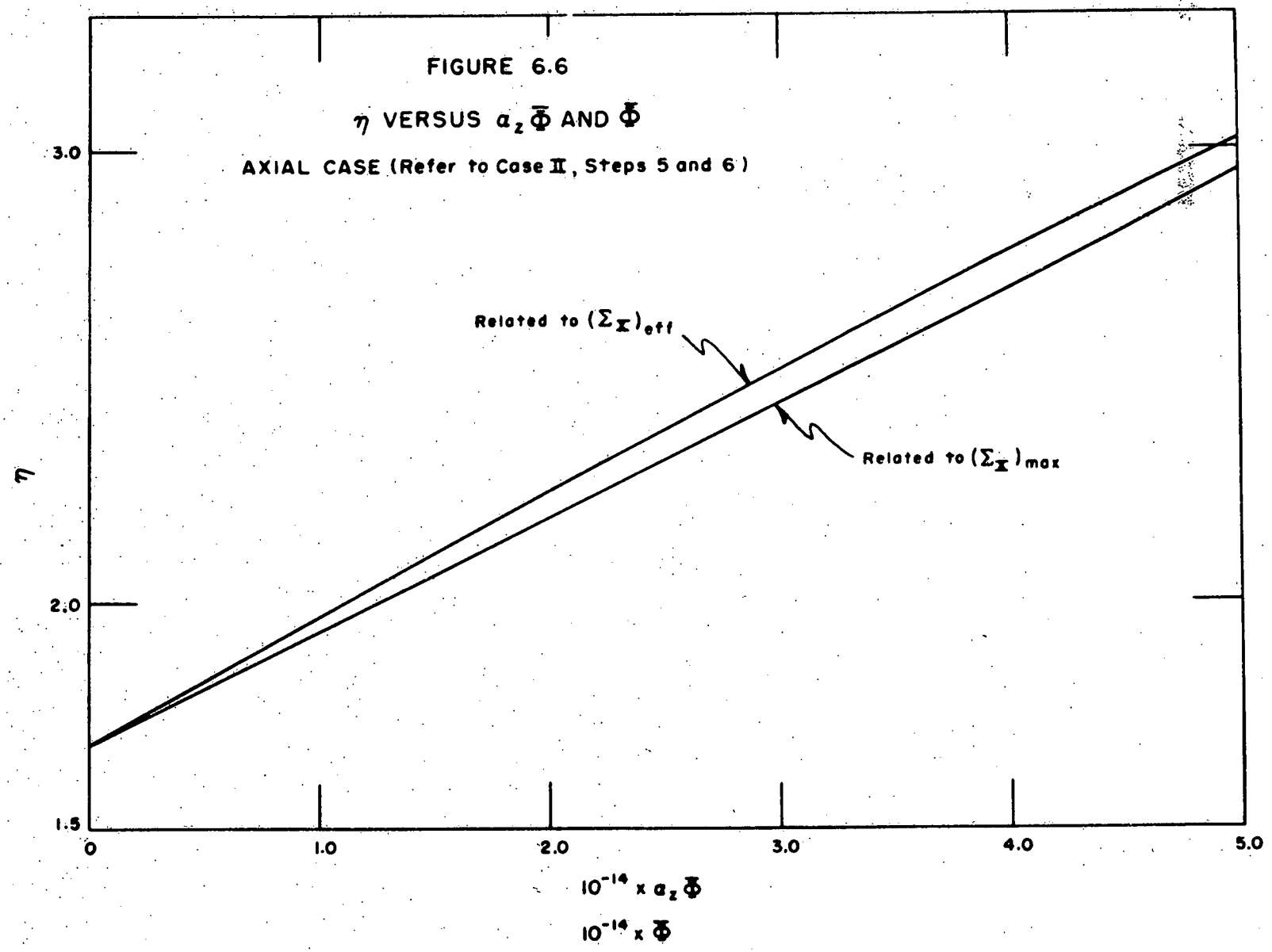

of η's in the functions of Figure 6.6 yields a functional relationship between α_z and $\bar{\Phi}$. The relationship α_z versus $\bar{\Phi}$ is pictured in Figure 6.7. The limiting value of α_z as $\bar{\Phi}$ tends to zero is obtained by the procedure described in Comment 2 under Case I.

Note once again that α_z is the over-all weighting factor associated with a xenon override problem for the special case where it is assumed that $\alpha_r = 1$.

Step 6a. Figure 6.8 is devoted to a graph of the preshutdown axial flux, $\mathcal{Z}(z)$, and graphs of the thermal axial flux at the time of xenon override, $Z(z)$, corresponding to a wide range of values of the preshutdown power level. Note that $Z(z)$ was thought to be essentially a cosine in character prior to the time that the present study was undertaken. Graphs of the fast fluxes, corresponding to the thermal fluxes of Figure 6.8, are exhibited in Figure 6.9.

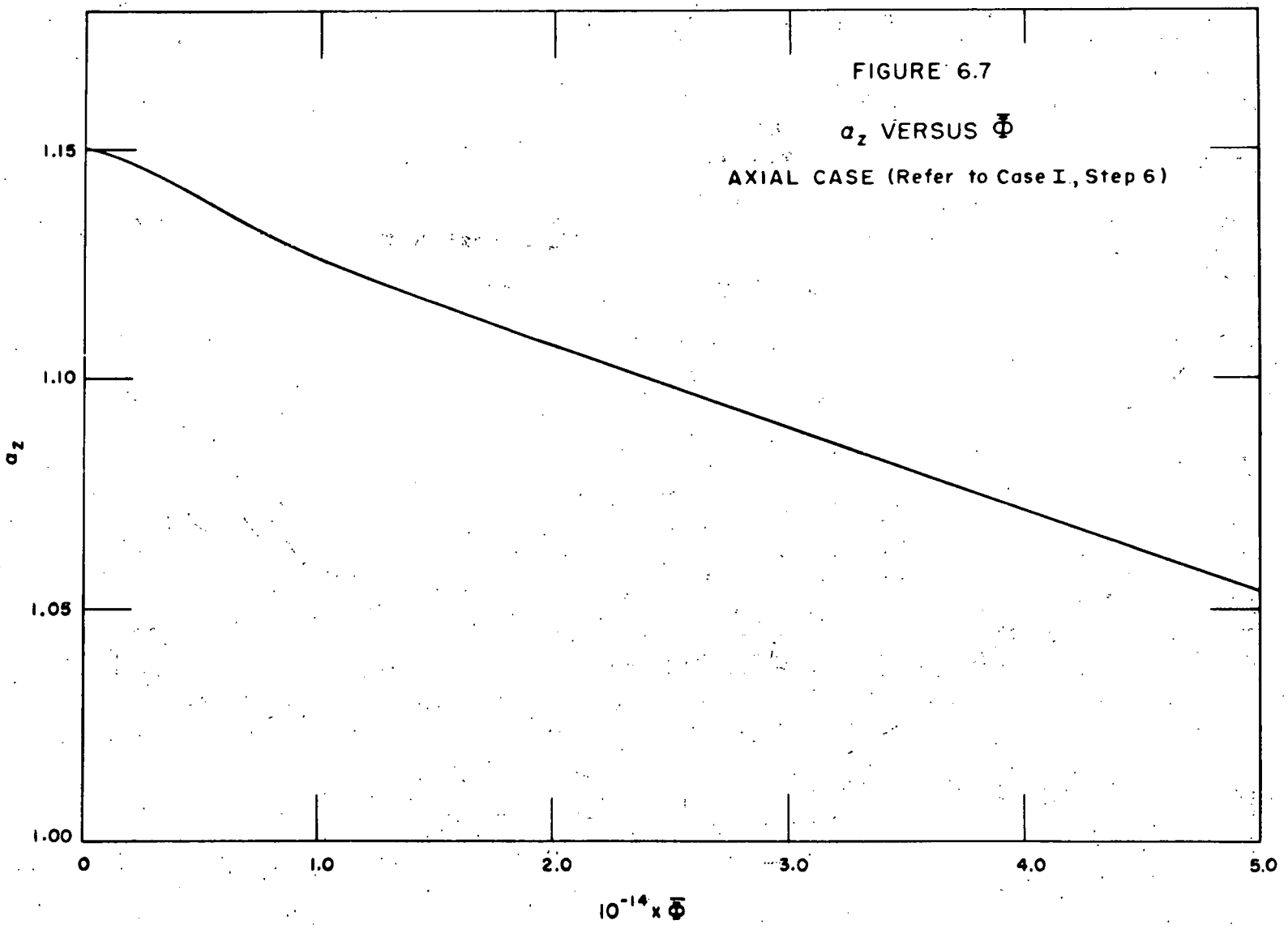

FIGURE 6.7

a_z VERSUS $\bar{\Phi}$

AXIAL CASE (Refer to Case I, Step 6)

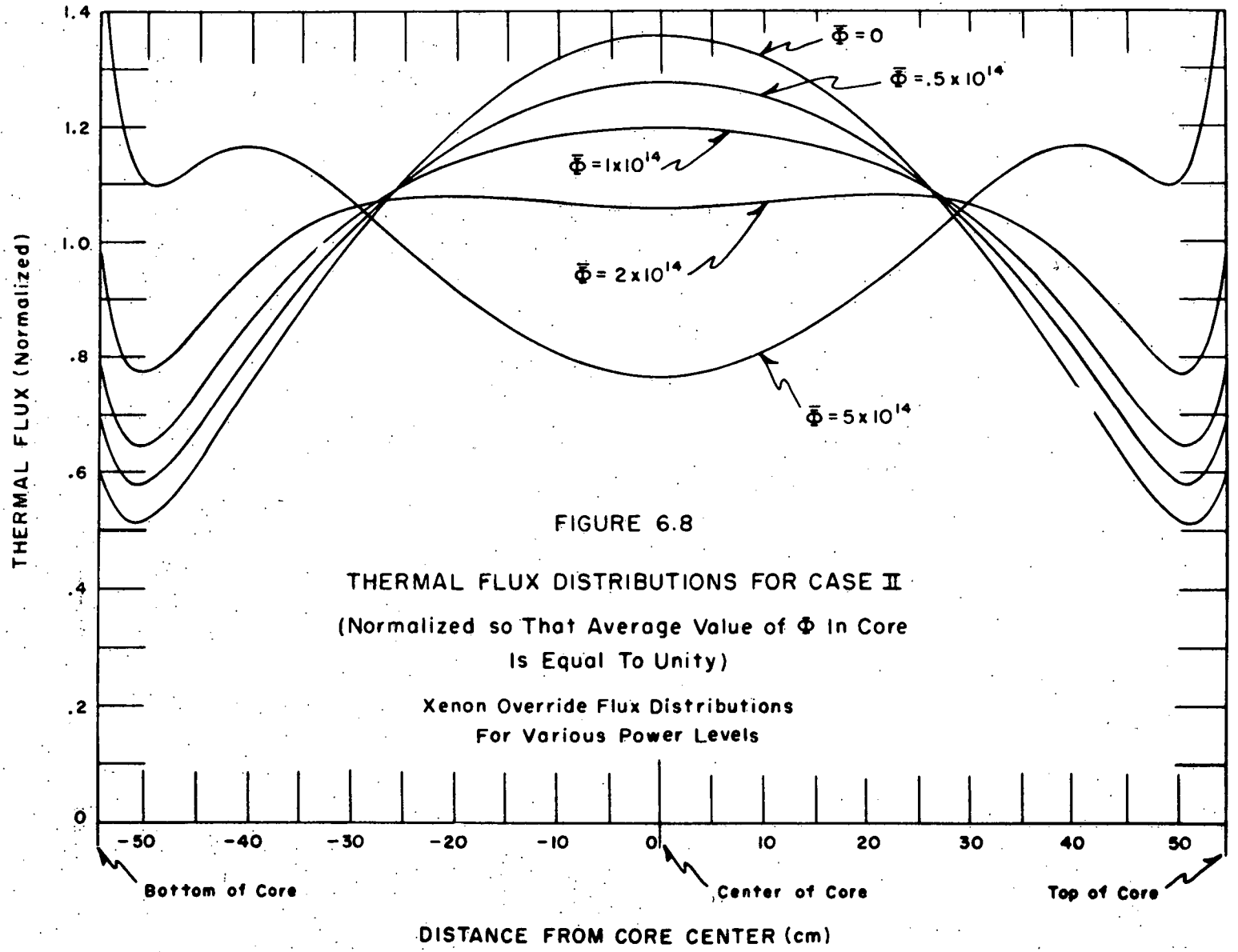

FIGURE 6.8

THERMAL FLUX DISTRIBUTIONS FOR CASE II

(Normalized so That Average Value of Φ In Core Is Equal To Unity)

Xenon Override Flux Distributions For Various Power Levels

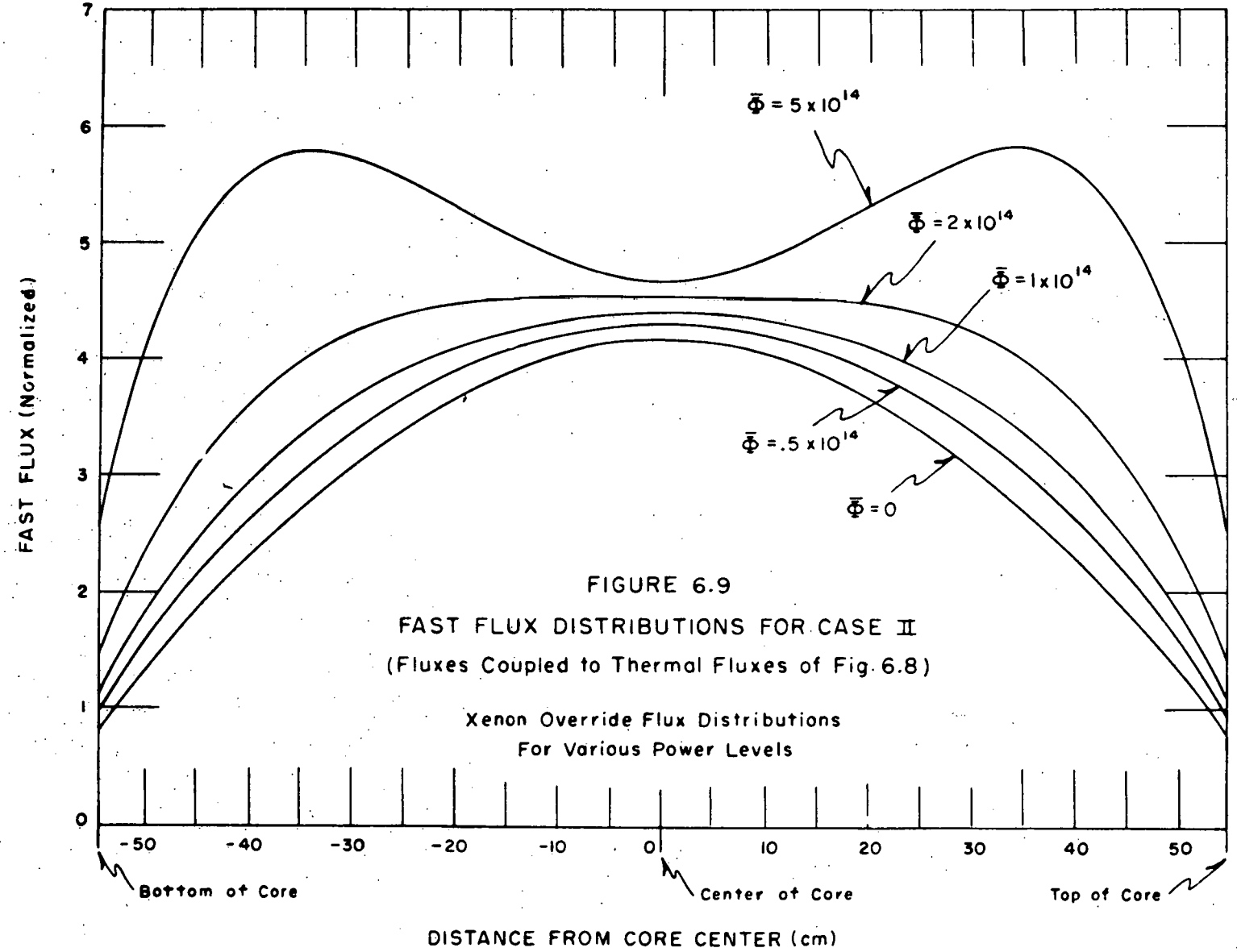

FIGURE 6.9

FAST FLUX DISTRIBUTIONS FOR CASE II

(Fluxes Coupled to Thermal Fluxes of Fig. 6.8)

☆ U. S. GOVERNMENT PRINTING OFFICE: 1956 O—372367